International Journal of Thermophysics, Vol. 15, No. 5, 1994

Thermal Diffusivity and Ultrasonic Velocity of Saturated R152a

K. Kraft[1] and A. Leipertz[1,2]

Received August 18, 1994

We report thermal diffusivity and ultrasonic sound velocity data for both phases of saturated difluorethane (R152a) in the temperature range from 278 K to the critical temperature. The data were obtained in thermodynamic equilibrium by applying dynamic light scattering. For both values comparison with data from literature has been made.

KEY WORDS: dynamic light scattering; R152a; refrigerants; sound velocity; thermal diffusivity.

1. INTRODUCTION

Strong efforts are necessary to provide useful data on the thermophysical properties of chlorine-free refrigerants to allow fast substitution of those refrigerants depleting the ozone layer. As no reference measurement system for data generation has been accepted so far, for a reliable database preferably data sources from several authors using different methods should be used. Dynamic light scattering (DLS) or photon-correlation spectroscopy (PCS) provides a useful supplement for data sets which have been obtained by traditional methods, e.g., by transient hot-wire measurements for thermal conductivity. In DLS no temperature or pressure gradients have to be applied on the sample, yielding absolute results without any necessary correction.

With the help of the measured thermal-diffusivity data the consistency of thermal conductivity, density, and isobaric heat capacity of one substance can be investigated. This allows an estimation of the accuracy of

[1] Lehrstuhl für Technische Thermodynamik, Universität Erlangen-Nürenberg, Am Weichselgarten 9, D-91058 Erlangen, Germany.

[2] To whom correspondence should be addressed.

0195-928X/94/0900-0791$07.00/0

these data sets. Additionally, the measured data of the sound velocity allow us to investigate the accuracy of values calculated with the help of a fundamental equation of state. This is done in this paper for the alternative refrigerant R152a.

2. METHOD

Dynamic light scattering (DLS) is a well-established method for the determination of the thermal diffusivity of fluids near the critical point (as the easiest application) as well as at much lower temperatures [1–3]. Recently, the method has also been applied to determine the ultrasonic sound velocity [4–9]. The experimental setup and the measurement procedure have been described in detail elsewhere [10, 11]. Here only the principle of the technique is indicated.

In a pure fluid, incident laser light is scattered by hydrodynamic modes in all directions. These modes exist in thermodynamic equilibrium of the fluid. The spectrum of the scattered light contains three lines (see Fig. 1), an unshifted Rayleigh line caused by entropy (temperature) fluctuations and two symmetrical shifted Brillouin lines which are caused by pressure fluctuations due to the Doppler effect (see, e.g., Ref. 12). The

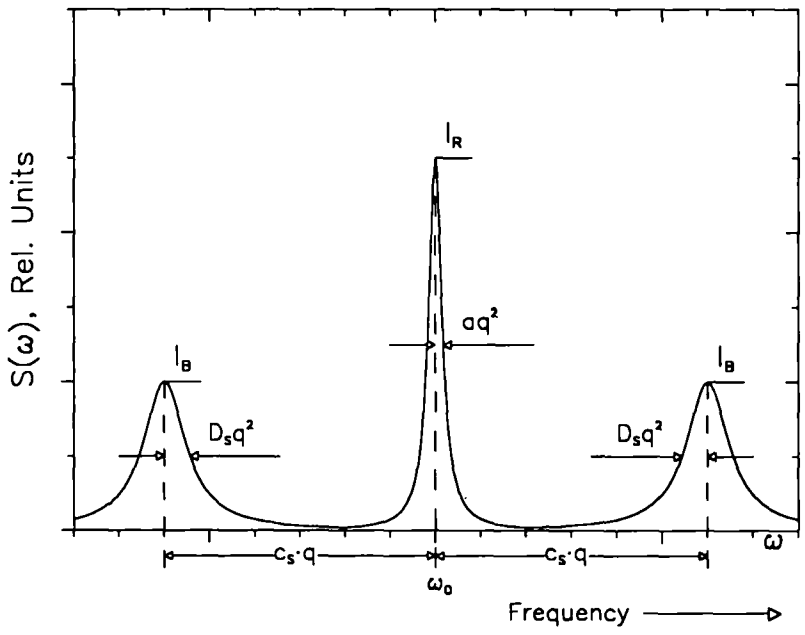

Fig. 1. Power spectral density of a pure fluid

spectral line widths of these different contributions depend on the modulus of the scattering vector q and on either the thermal diffusivity a for the unshifted Rayleigh line or the sound attenuation constant D_S for the shifted Brillouin lines. For a small observation angle Θ_e, q can be calculated from this angle and the laser wavelength λ_0 [3]

$$q = \frac{2\pi \sin \Theta_e}{\lambda_0} \tag{1}$$

The line widths are given by

$$\delta\omega_R = aq^2 \tag{2}$$

and

$$\delta\omega_B = D_s q^2 \tag{3}$$

for the Rayleigh and Brillouin lines, respectively. The sound velocity c_S can be calculated from the frequency shift of the Brillouin lines relative to the laser frequency by

$$\Delta\omega_B = |\omega_B - \omega_0| = c_s q \tag{4}$$

The very narrow lines usually cannot be resolved in the frequency domain by available spectrometers as, e.g., Fabry-Perot interferometers. Thus, the determination of the line width has to be done in the time domain using DLS [13].

In DLS the correlation function of the scattered light intensities is calculated, which is the inverse Fourier transform of the frequency spectrum. For the determination of the thermal diffusivity one part of the incident laser light (reference light) is superimposed to the scattered light from the probe (heterodyne technique). In this case, for pure fluids from the Rayleight signal a single exponentially decaying correlation function is obtained. From the decay time, which is inversely proportional to the Rayleigh line width, the thermal diffusivity can be calculated according to Eq. (2).

To determine the sound velocity, the frequency shift of the Brillouin lines is measured. For this, the reference light, which is superimposed to the scattered light, is frequency shifted by means of an acousto optical modulator. If the frequency difference between the reference light and the Brillouin signal is not too high, a damped oscillation, which is generated from the beating of both contributions, is measured. From the frequency of this oscillation and the shift of the reference light, the sound velocity can be calculated according to Eq. (4) [9, 10].

In all experiments, the sample remains in thermodynamic equilibrium with coexisting vapor and liquid phases. Which of both phases is measured can be chosen simply by the height of the incident laser beam passing the sample cell. The sample temperature is measured by means of a calibrated Pt100 probe with an accuracy of 50 mK.

Based on error analysis, the overall system accuracy for the thermal diffusivity and the sound velocity has been estimated to be within ± 3 and $\pm 0.5\%$, respectively, for a single measurement. These values include already the errors of the angle measurement and of the data evaluation procedure. To this value the temperature error must be added according to the thermodynamic state of the sample [10].

3. RESULTS AND DISCUSSION

Prior to the measurements the refrigerant was filtered and cleaned to remove high boiling fractions and water. The analysis after the cleaning process indicated a purity of better than 99.8%, which is the resolution of the used analysis system (Perkin Elmer Q-Mass 910) based on gas chromatography and mass spectrometry.

3.1. Thermal Diffusivity

The thermal diffusivity of R152a has been measured along the saturation line. The results are given in Table I and are displayed in Fig. 2. In no case was a correlation found between the laser power and the measured thermal diffusivity. This indicates that the dissipated laser energy was neglegible even near the gas liquid critical point.

In the literature two reference data sets can be found providing measurement results on the thermal diffusivity of liquid R152a [14, 15]. Figure 3 gives a comparison of all three data sets. The temperature dependence of our results is similar to that found by Gross et al. [14] within the common temperature range investigated. The absolute values are nearly 5% lower, which is typical for DLS data in comparison to data measured by more conventional techniques such as the transient hot-strip method used by Gross et al. The accuracy of these results is estimated to be within 3 to 4%. Taking into account our estimated measurement accuracy, the difference between both data sets is well within the accumulated inaccuracies of both techniques used.

Ibreighith et al. [15] used the same measurement technique as ours. Near room temperature their results agree with ours within the estimated inaccuracy of the techniques. For higher temperatures the data of Ibreighith et al. are systematically larger and also differ in their temperature

Table I. Thermal Diffusivity of Saturated R152a

Temperature (°C)	a (10^{-8} m^2·s^{-1})
(a) Liquid phase	
5.54	6.69
15.58	6.43
25.67	6.14
35.53	5.82
45.59	5.51
55.72	5.20
65.73	4.93
75.80	4.54
85.91	4.07
95.93	3.46
106.05	2.24
108.58	1.73
110.07	1.35
111.59	0.860
111.58	0.858
112.61	0.475
(b) Vapor phase	
86.94	10.2
92.00	8.30
97.05	6.42
102.02	4.61
110.12	1.54
112.67	0.492

dependence. We are not able to explain this difference, in particular, not as the results of R142b given in the same paper agree with out results within $\pm 1\%$ over the entire temperature range [11]. We assume that the substance under investigation was different in its chemical composition, which has not been proved analytically for the former measurements [15].

A comparison with the results of the thermal conductivity λ in the literature can be done by using available data for the density ρ and the isobaric heat capacity c_p. For the saturated liquid available data sources for density (Refs. 16–21 and references therein) and isobaric heat capacity [22, 23] show a consistency of 0.5% for the density and 1% for the isobaric heat capacity.

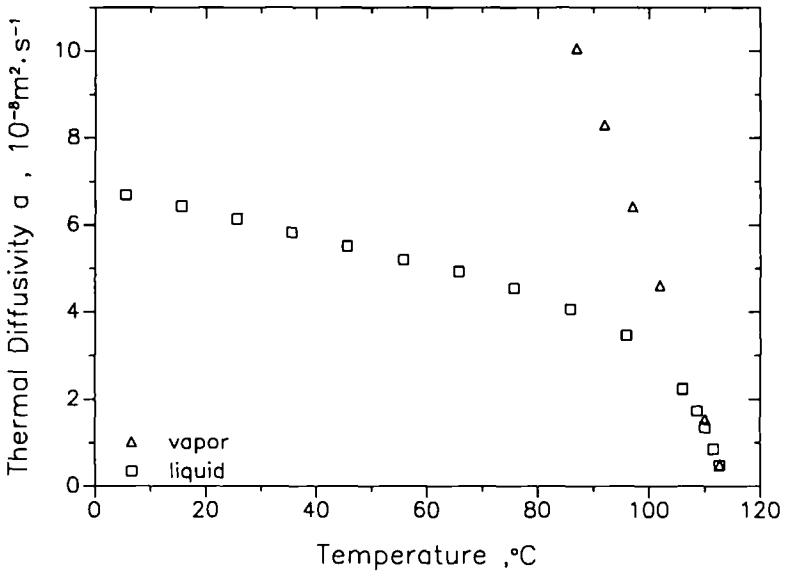

Fig. 2. Thermal diffusivity of saturated R152a.

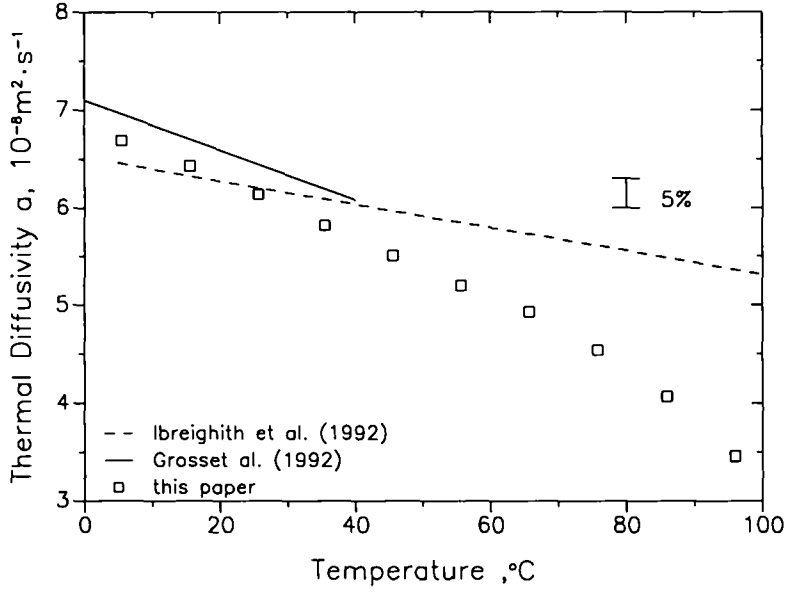

Fig. 3. Thermal diffusivity of liquid saturated R152a measured by different authors.

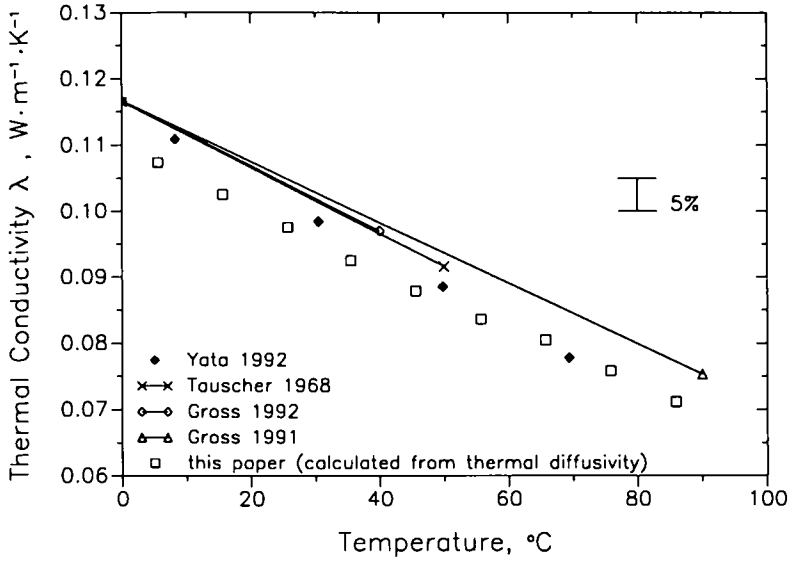

Fig. 4. Thermal conductivity of liquid saturated R152a measured by different authors.

In Fig. 4 the thermal conductivity of the saturated liquid measured by different authors [24–26] is compared with our data, which have been transformed into the thermal conductivity by

$$\lambda = a\rho c_p \tag{5}$$

with the isobaric heat capacity measured by Nakagawa [22] and the density proposed by McLinden [20]. All data sets are found to be consistent within $\pm 2.5\%$. For low temperatures, the results of Gross, Tauscher, and Yata are consistently 5% higher than the values calculated from our thermal-diffusivity data, which is often found when comparing DLS data with those gained by methods applying a temperature gradient on the sample. For higher temperatures, the results of Yata approach our values, while the thermal conductivity given by Gross remains above these values by approximately 3%.

3.2. Sound Velocity

The results for the ultrasonic sound velocity of R152a on the saturation line are given in Table II and are shown in Fig. 5. The measured frequencies cover the range from 80 MHz for the lowest temperature down to 10 MHz near the critical point [10].

Table II. Sound Velocity of Saturated R152a

Temperature (°C)	c_s ($m \cdot s^{-1}$)
(a) Liquid phase	
5.55	743
15.59	692
25.67	642
35.52	596
45.57	542
55.69	490
65.72	435
75.79	382
85.85	321
95.94	256.2
106.05	180.8
108.56	158.6
110.08	144.3
111.56	127.6
112.62	115.4
(b) Vapor phase	
86.94	155.8
92.00	151.0
97.04	145.5
102.03	139.6
110.12	125.6
112.68	117.3

Especially near the critical point a frequency dependence of the sound velocity (dispersion) can occur. In Fig. 6 the measured sound velocity of the saturated liquid at 106°C is shown as function of the frequency. A linear regression to zero frequency yields a correction of the average value of about 0.5%. However, all measured values are very well within the estimated inaccuracy, so no frequency correction is neccessary.

At the moment no measured values of the sound velocity for R152a can be found in the literature. However, with the aid of a fundamental equation of state (EOS), a comparison between calculated and measured values can be performed. A fundamental equation of state for R152a has been developed by Tillner-Roth [27], which is not based on measured sound velocity data.

Figure 7 displays the deviation of our results from the calculated values of the sound velocity using the EOS [27]. In the liquid phase we find an agreement within $\pm 0.5\%$ between our data and the calculated

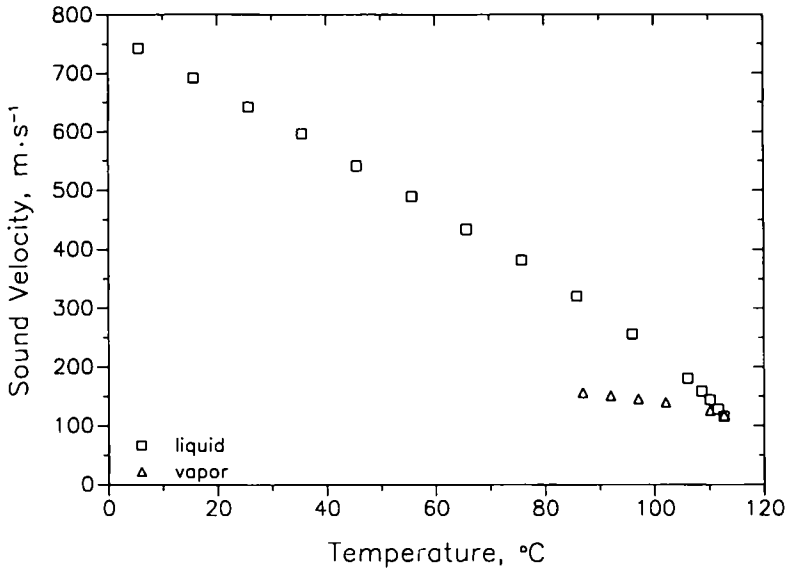

Fig. 5. Ultrasonic sound velocity of saturated R152a.

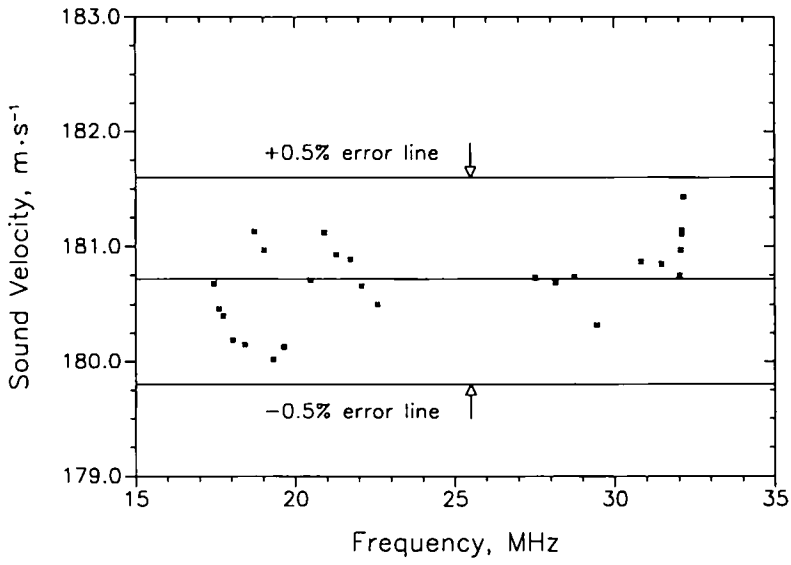

Fig. 6. Frequency dependence of saturated liquid sound velocity at 106 °C.

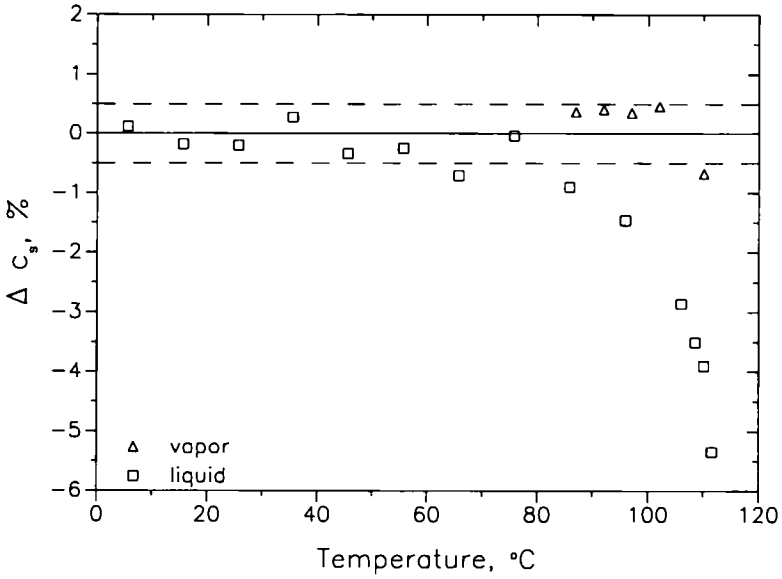

Fig. 7. Comparison of measured and calculated sound velocity of saturated R152a.

values for temperatures up to 80 C. This indicates a good reliability of the thermal and caloric data sets of this refrigerant for this temperature range and of the DLS technique as a measurement method for the determination of the sound velocity. The obvious deviations when approaching the critical point may be caused by the lack of caloric data for setting up the fundamental equation of state. Here only one data set of isobaric heat capacity in compressed liquid is available [23], showing strong deviations between measurement and calculation, in particular near the critical point [28].

4. CONCLUSION

In this paper, thermal-diffusivity data for both phases are provided also near the critical point, extending the range of available data sets. A comparison with thermal-conductivity data of liquid saturated R152a in the temperature range from room temperature up to 90 C shows that the available data sources give higher thermal conductivity values than we have found when converting our thermal-diffusivity data. The obtained difference is bigger than the estimated inaccuracy of the measurements and the additional error from data conversion from thermal diffusivity to thermal conductivity predicts. This situation is still unsatisfactory and may be cleared by further measurements.

The sound velocity data presented in this paper are the first available for this refrigerant. These data can help to improve future equations of state, in particular near the critical point.

ACKNOWLEDGMENTS

The authors gratefully acknowledge financial support by the Deutsche Forschungsgemeinschaft. We also thank Solvay Fluor and Derivate GmbH and Du Pont de Nemours for providing us with refrigerant R152a and D. Bernt and R. Eckstein (Lehrstuhl Technische Chemie II; Prof. Steiner) for analyzing the purity of the refined refrigerant.

REFERENCES

1. A. Leipertz, *Int. J. Thermophys.* **9**:897 (1988).
2. M. Hendrix, A. Leipertz, M. Fiebig, and G. Simonsohn, *Int. J. Heat Mass Transfer* **30**:333 (1987).
3. M. Hendrix, *Photonen-Korrelationsspektroskopie als optisches Standardverfahren zur Messung der Temperaturleitfähigkeit reiner Flüssigkeiten in einem weiten Temperatur- und Druckbereich*, Dr-Dissertation (Ruhr-Universität Bochum, 1984).
4. B. Hinz, G. Simonsohn, M. Hendrix, G. Wu, and A. Leipertz, *J. Modern Opt.* **34**:1093 (1987).
5. G. Simonsohn and F. Wagner, *Opt. Lett.* **14**:110 (1989).
6. G. Simonsohn and F. Wagner, *J. Phys. D Appl. Phys.* **22**:1179 (1989).
7. A. Leipertz, K. Kraft, and G. Simonsohn, *Fluid Phase Equil.* **79**:201 (1992).
8. G. Simonsohn, *Opt. Acta* **30**:1675 (1983).
9. K. Kraft and A. Leipertz, *Appl. Opt.* **32**:3886 (1993).
10. K. Kraft and A. Leipertz, *Int. J. Thermophys.* **15**: 387 (1994).
11. K. Kraft, S. Will, and A. Leipertz, *Measurement* (1994), in press.
12. B. J. Berne and R. Pecora, *Dynamic Light Scattering* (Wiley, New York, 1976).
13. M. Hendrix and A. Leipertz, *Phys. unserer Zeit* **15**:68 (1984).
14. U. Grosss, Y. W. Song, and E. Hahne, *Fluid Phase Equil.* **76**:273 (1992).
15. M. Ibreighith, M. Fiebig, A. Leipertz, and G. Wu, *Fluid Phase Equil.* **80**:323 (1992).
16. Y. Higashi, M. Ashizawa, Y. Kabata, T. Majima, M. Uematsu, and K. Watanabe, *JSME Int. J.* **30**:1106 (1987).
17. R. Tillner-Roth, H. D. Baehr, and F. Klobasa, *Kälte-Klima-Tagung* (Heidelberg, 1990), Vol. 2, p. 193.
18. A. Kamei, C.-C. Piao, H. Sato, and K. Watanabe, *ASHRAE Trans.* **96** (1990), Part. 1, p. 141.
19. ASHRAE, *ASHRAE Handbook Fundamentals* (ASHRAE, Atlanta, 1986).
20. M. O. McLinden, *Rev. Int. Froid* **13**:149 (1990).
21. M. O. McLinden, *World Meteorological Organization; Global Ozon Research and Monitoring Project*, Report No. 20, Vol. II (1989).
22. S. Nakagawa, T. Hori, H. Sato, and K. Watanabe, *J. Chem. Eng. Ddata* **38**:70 (1993).
23. E. G. Porichanskii, O. P. Pompmareva, and P. I. Svetlichnyi, *Izv. Vys. Ucheb. Zaved. Energ.* **3**:122 (1982).
24. U. Gross, Y. W. Song, Y. W. Kellebenz, and E. Hahne, *DKV Tagungsbericht* (Berlin, 1991), p. 239.

25. W. Tauscher, *Wärme- Stoffübertragung* **1**:140 (1968).
26. J. Yata, M. Hori, T. Kurahashi, and T. Minamiyama, *Fluid Phase Equil.* **80**:287 (1992).
27. R. Tillner-Roth, personal communication (University of Hannover, Hannover, 1993).
28. R. Tillner-Roth, *Forschungsberichte des Deutschen Kälte- und Klimatechnischen Vereins* No. 41 (1993).